Facile Development of Superparamagnetic Nanoparticle Encapsulated Protein based Nanocarrier for Targeted Drug Delivery Application

Khushnuma Asghar, Mohd Qasim and Dibakar Das[a]

School of Engineering Sciences and Technology, University of Hyderabad, Hyderabad 500046, India
[a)] Corresponding author: ddse@uohyd.ernet

Abstract. In this work, facile development of superparamagnetic Fe_3O_4 nanoparticle encapsulated bovine serum albumin (BSA) based nanocarrier (Fe_3O_4@BSA) for targeted drug delivery application has been reported. First, highly monodisperse and well crystalline superparamagnetic Fe_3O_4 nanoparticle was prepared and then a green and simple sonochemical method was used for the development of Fe_3O_4@BSA nanocarrier. The structural, morphological, and magnetic properties of the prepared Fe_3O_4@BSA nanocarrier have been studied by XRD, TEM, SAED, FTIR and VSM techniques. The particle sizes of Fe_3O_4 nanoparticle and Fe_3O_4@BSA nanocarrier were found to be 5-10 nm and 50-300 nm respectively. TEM micrographs and FTIR analysis confirmed the successful coating of amorphous BSA on crystalline Fe_3O_4 NPs. Magnetic measurement revealed the superparamagnetic nature of the prepared Fe_3O_4@BSA nanocarrier. Fe_3O_4@BSA nanocarrier with smaller particle sizes, good physical and chemical stability, excellent water dispersability and low toxicity could have potential for targeted drug delivery applications.

INTRODUCTION

Magnetic nanoparticles (MNP), particularly superparamagnetic Fe_3O_4 NP are receiving increasing attention for various biological applications including targeted drug delivery, magnetic bio-separation, hyperthermia and MRI due to its excellent magnetic properties and proven biocompatibility [1]. For most of the biomedical applications a stable aqueous suspension of MNPs is required, however, due to their high surface energy and dipolar interaction MNPs tend to aggregate into larger cluster when subjected to the biological or aqueous media. To prevent surface aggregation, faster degradation of bare Fe_3O_4 nanoparticles, to reduce uptake of Fe_3O_4 by retieculo-endothelium system, and to incorporate drug loading ability it is essential to modify nanoparticles surface with biocompatible hydrophilic and biodegradable materials. Various polymers such as PEG, PLGA, Dextran, P(NIPam-Am), and protein have been coated onto Fe_3O_4 NP surface to achieve efficient stability, targeting and controlled drug delivery [2]. Recently, fabrication of protein coated MNPs based nanocarriers have attracted significant attention due to its exceptional biocompatibility, biodegradability and water dispersibility. Among several types of proteins, bovine serum albumin (BSA) based magnetic nanocarriers have been considered as an ideal material for efficient therapeutic application due to its hydrophilic and biocompatible nature. BSA coated magnetic nanoparticles have been prepared by various routes and chemical method employing a crosslinker molecule is very common [3,4]. However, ultra-sonication based method which does not require any cross-linker is environmental friendly thus does not leave any undesired toxic residue [5]. Nowadays green chemistry is the focus of pharma industries due to its inexpensive and environmentally superior nature. In the present work, a biocompatible, non-toxic, biodegradable, hydrophilic, inexpensive and magnetically guidable BSA coated Fe_3O_4 NP (Fe_3O_4@BSA) based magnetic protein nanocarrier has been successfully synthesized by green and simple sonochemical method for targeted and controlled drug delivery and has been characterized for structural, morphological and magnetic properties.

EXPERIMENTAL

Well crystalline and monodispersed Fe_3O_4 NPs were prepared by co-precipitation of ferric and ferrous salts in presence of NaOH and oleic acid in aqueous media. In a typical synthesis procedure, first $FeCl_3$ and $FeCl_2$ (in 2:1 molar ratio) were dissolved in 120 ml of distilled water. Then the solution was magnetically stirred for 30 minutes and 2 gm of NaOH (dissolved in 30 ml water) was added to the above solution. It was followed by the addition of 2 ml of oleic acid as capping agent. The dark brown color solution so obtained was further stirred for about two hours. Throughout the stirring the reaction temperature was maintained at 80°C. The obtained brown precipitates were magnetically separated, washed and dried at 100 °C to obtain Fe_3O_4 NPs. To prepare Fe_3O_4@BSA nanocarriers, first appropriate amount of prepared Fe_3O_4 NPs was dispersed in 8 ml of distilled water by ultrasonication and then 2 ml of BSA aqueous solution (250 mg/ml) was added slowly to the Fe_3O_4 NPs homogeneous dispersion with continuous ultrasonication. The obtained Fe_3O_4 and BSA mixture was further ultra-sonicated for 30 min and then subjected to magnetic stirring for ~3 h. The resultant Fe_3O_4@BSA nanocarriers were magnetically separated, washed and stored in glass vial for characterization. Schematic diagram for formation mechanism of Fe_3O_4 NPs and Fe_3O_4@BSA nanocarriers are shown in figure 1 (a).The crystalline structure of Fe_3O_4@BSA nanocarriers was characterized by a Bruker D8 Advance X-ray diffractometer. The morphology and particle size of Fe_3O_4 NP and Fe_3O_4@BSA nanocarrier were analyzed by using TEM (FEI Tecnai T20G2 S TWIN TEM). The magnetic property of Fe_3O_4@BSA nanocarrier was studied using a Lakeshore (Model 7407) VSM. The chemical structure and functional groups of samples were analyzed using a PerkinElmer 2000 FT-IR spectrometer.

RESULTS AND DISCUSION

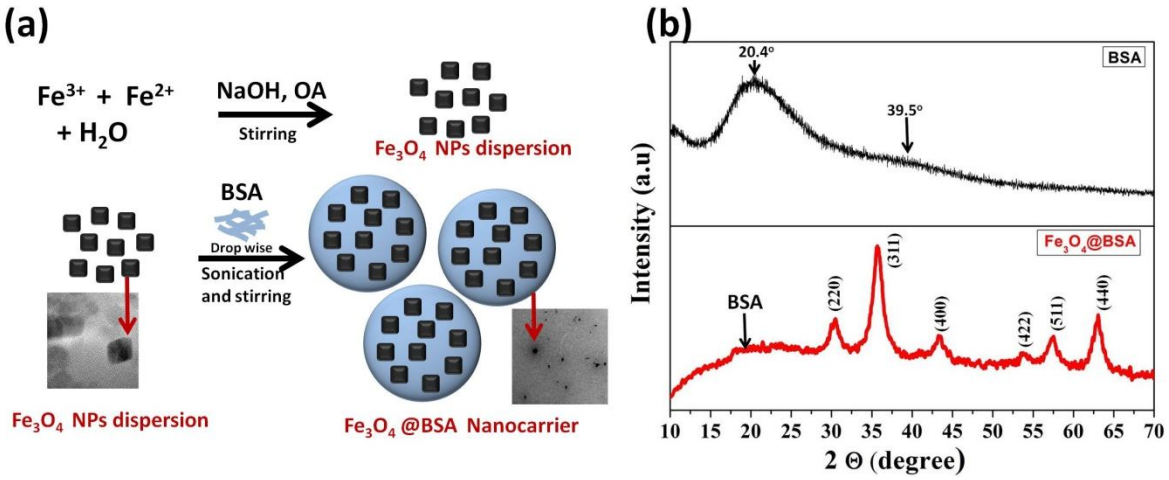

FIGURE 1. (a) Schematic diagram showing formation mechanism of Fe_3O_4 NPs and Fe_3O_4@BSA nanocarriers. (b) XRD patterns of pure BSA powder and Fe_3O_4@BSA nanocarrier.

Presence of crystalline Fe_3O_4 NP in amorphous BSA matrix was examined by powder XRD technique. Fig. 1(b) shows the XRD patterns of pure BSA powder and Fe_3O_4@BSA nanocarrier. The XRD pattern of pure BSA shows the presence of two broad non diffraction peaks around 2Θ 20.4° and 39.5°, which can be attributed to amorphous nature of BSA. XRD pattern of Fe_3O_4@BSA nanocarrier shows a broad hump at ~20.4° with few sharp diffraction peaks at 2 Θ 30.4°, 35.7°, 43.2°, 53.6°,57.2° and 63.0° (fig. 1 (b) (bottom panel). The broad hump at 20.4° can be attributed to the amorphous BSA matrix, whereas all the sharp diffraction peaks can be assigned to the reflections originated from the planes (220), (311), (400), (422), (511) and (440) respectively of spinal cubic Fe_3O_4 NPs. The obtained diffraction peaks correlate well with the standard values for the spinal cubic Fe_3O_4 (JCPDS cards No. 88-315). The crystallite size of Fe_3O_4 NP in the nanocomposite was estimated using Debye–Scherrer equation and was found to be ~ 5.5 nm. Appearance of characteristic diffraction peaks of both BSA and Fe_3O_4 in XRD pattern of Fe_3O_4@BSA nanocarrier indicated the successful formation of Fe3O4@BSA nanocarrier.

The structure and morphology of the prepared Fe_3O_4 NP and Fe_3O_4 @BSA nanocarrier were studied using TEM. Fig. 2 (a-b) shows the TEM (a) and HRTEM (b) micrographs of Fe_3O_4 NP. In TEM micrographs of Fe_3O_4 NP nearly uniformly distributed square shape Fe_3O_4 NP can be observed. The particle size of Fe_3O_4 NPs was found to be ~5-10

nm. In HRTEM image of Fe_3O_4 NP, appearance of ordered lattice fringes indicated the formation of well crystalline Fe_3O_4 NP. Inverse fast Fourier transform (IFFT) image (fig 2 (c)) for selected region of HRTEM micrograph of Fe_3O_4 NP shows ordered planes with d spacing of ~ 0.3 nm, which corresponds to (220) plane of Fe_3O_4 NPs. Fig. 2 (d-f) shows the TEM images of Fe_3O_4@BSA nanocarriers at different magnifications. It was observed that many smaller Fe_3O_4 NPs (particle size 5-10 nm) were incorporated within the BSA matrix to form larger size (~50-300 nm) Fe_3O_4@BSA nanocarrier having irregular morphology. Coating of BSA (light grey color layer) on Fe_3O_4 NPs (black color particles) is clearly visible in low and high magnification TEM images (fig 2 (d-f)). Thickness of BSA coating is found to be ~ 20-150 nm. The indexed SAED patterns of Fe_3O_4@ BSA nanocarrier (inset of fig 2(d)) show the presence of characteristic distinct ring pattern of spinel cubic Fe_3O_4 NPs, which also confirms the presence of polycrystalline Fe_3O_4 NPs in Fe_3O_4@BSA nanocarrier.

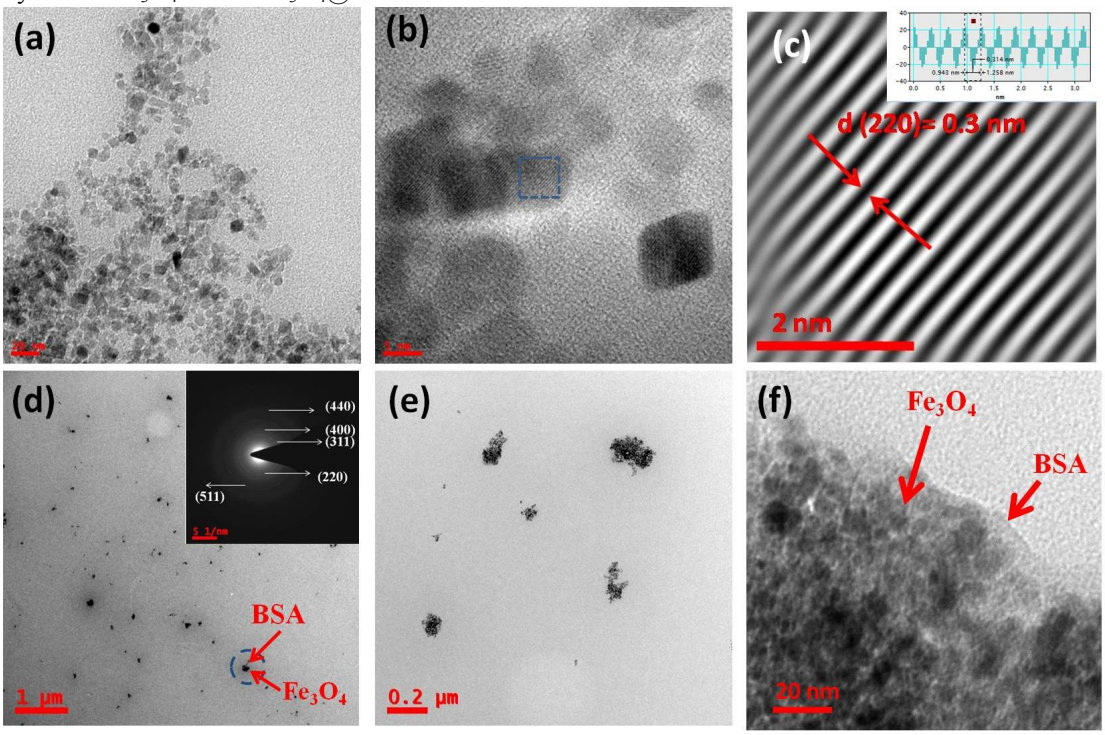

FIGURE 2. (a) TEM and (b) HRTEM micrographs of Fe_3O_4 NPs. (c) IFFT image for selected region (blue color) of fig 2(b). Line profile through atomic planes is shown in inset of fig (c). (d-f) TEM micrographs of Fe_3O_4@BSA nanocarrier at different magnifications. Indexed SAED pattern of Fe_3O_4@BSA nanocarrier is shown in inset of figure 2 (d).

Further confirmation about the formation of the Fe_3O_4@BSA nanocarrier was made by FTIR analysis of pure BSA and Fe_3O_4@BSA nanocarrier. Fig. 3(a) shows the FTIR spectra of pure BSA and Fe_3O_4@BSA nanocarrier. The spectra of pure BSA (figure 3 (a)(top)) shows only characteristic absorption bands of BSA which showed its high purity level. The characteristics absorption bands of BSA appeared at 1658, 1535 and 1238 cm-1, which were assigned to the vibrations of C=O stretching (amide I), C-N stretching (amide II) and C-H stretching + N-H bending (amide III), respectively [6]. The broad absorption bands at 3380 cm-1 can be attributed to the stretching vibration of N-H (amide I). IR spectra of Fe_3O_4@BSA nanocarrier showed the presence of all the characteristics absorption bands of BSA with additional few new characteristic absorption bands from Fe_3O_4 NPs. The additional absorption bands at 633 and 558 cm^{-1} were attributed to the vibration of Fe-O bond stretching [2]. Thus, the simultaneous presence of characteristic bands of both Fe_3O_4 and BSA in the IR spectra of Fe_3O_4@BSA nanocarrier indicated the successful formation of Fe_3O_4@BSA nanocarrier.

The magnetic properties of Fe_3O_4@BSA nanocarrier was studied by vibrating sample magnetometer at room temperature (RT). Fig. 3(b) shows the magnetization (M) versus applied magnetic field (H) hysteresis curve of Fe_3O_4@BSA nanocarrier measured in the applied field between -1.5 and 1.5 T at RT. The absence of hysteresis loop indicated the superparamagnetic nature of the prepared Fe_3O_4@BSA nanocarrier with negligible coercivity (Hc) and remnant magnetization (M_R). For biomedical applications especially for targeted drug delivery, superparamagnetic nature of magnetic nanocarrier is required to avoid aggregation of nanocarriers by magnetic attractions. The maximum magnetization (M) value at 1.5 T was found to be ~14 emu/g, which is sufficient for magnetically

targeted drug delivery applications. The Hc and M_R values were found to be 1.01 Oe and 0.01emu/gm, respectively (inset at the bottom of Fig. 3 (b)). Digital photographs of aqueous dispersion of Fe_3O_4@BSA nanocarrier in absence (A) and presence (B) of magnet are shown in inset of fig 3 (b) (top). Fe_3O_4@BSA nanocarriers were found to be highly water dispersible and magnetically targetable.

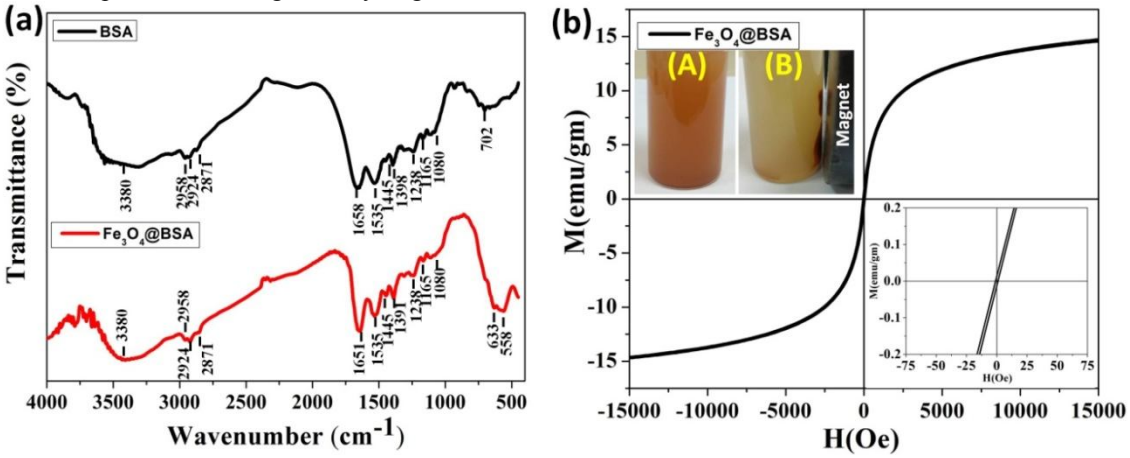

FIGURE 3. (a) FTIR patterns of pure BSA and Fe_3O_4@BSA nanocarrier. (b) Room temperature M-H curve of Fe_3O_4@BSA nanocarrier. Inset at the top of fig. (b) shows aqueous dispersion of Fe_3O_4@BSA nanocarrier, (A) without magnet and (B) with magnet. Inset at the bottom of fig. (b) shows enlarged M-H curve of Fe_3O_4@BSA nanocarrier.

Thus, these observed properties of prepared Fe_3O_4@BSA nanocarrier indicates that Fe_3O_4 and BSA based nanocarrier could find tremendous application in biomedical field. In addition, in depth investigation on suitability of Fe_3O_4@BSA nanocarrier for drug delivery application is underway which will further provide its real potential in targeted drug delivery application.

CONCLUSIONS

In conclusion, we have successfully synthesized biocompatible, biodegradable, hydrophilic, inexpensive and magnetically guidable Fe_3O_4@BSA nanocarrier by simple and eco-friendly sonochemical method without employing any crosslinking agent. The structural, morphological and magnetic properties of prepared Fe_3O_4@BSA nanocarrier were studied by different techniques. The particle size of the obtained Fe_3O_4@BSA nanocarrier was found to be ~ 50-300 nm. The prepared Fe_3O_4@BSA nanocarrier could be very much suitable and inexpensive candidate for targeted drug delivery, hyperthermia and MRI applications.

ACKNOWLEDGMENTS

Khushnuma Asghar greatly acknowledges the financial support obtained from the University Grants Commission (UGC) in the form of MANF fellowship (2014-15/MANF-2014-15-MUS-BIH-42040).

REFERENCES

1. M. Rahimi, A. Wadajkar, K. Subramanian, M. Yousef, W. Cui, J. Hsieh, K. Nguyen, Nanomedicine **6**, 672–680 (2010)
2. K Asghar, M Qasim, G Dharmapuri and D Das, RSC Adv. 7, 28802–18, (2017)
3. M. Bellusci, A. La Barbera, L. Seralessandri, F. Padella, A. Piozzi, F. Varsano, Polymer International **58** (10) 1142-1147 (2009)
4. Z. Li, L. Qiang, S. Zhong, H. Wang, X. Cui, Colloids and Surfaces A: Physicochemical and Engineering Aspects, **436** 1145-1151 (2013)
5. M Qasim, K Asghar, G Dharmapuri and D Das, Nanotechnology **28**, 365101 (2017)
6. Bronze-Uhle ES, Costa BC, Ximenes VF, Lisboa-Filho PN, Nanotechnology, Science and Applications, **10** 11–21 (2017)